The $(2+1)$-d $U(1)$ Quantum Link Model Masquerading as Deconfined Criticality*

D. Banerjee[1], F.-J. Jiang[2], P. Widmer[1], and U.-J. Wiese[1,3]
[1] *Albert Einstein Center, Institute for Theoretical Physics, Bern University, Switzerland*
[2] *Department of Physics, National Taiwan Normal University 88, Sec. 4, Ting-Chou Rd., Taipei 116, Taiwan*
[3] *Center for Theoretical Physics, Massachusetts Institute of Technology, Cambridge, Massachusetts, U.S.A.*

* **Dedicated to the memory of Bernard B. Beard (1957-2012)**

The $(2+1)$-d $U(1)$ quantum link model is a gauge theory, amenable to quantum simulation, with a spontaneously broken $SO(2)$ symmetry emerging at a quantum phase transition. Its low-energy physics is described by a $(2+1)$-d $\mathbb{R}P(1)$ effective field theory, perturbed by a dangerously irrelevant $SO(2)$ breaking operator, which prevents the interpretation of the emergent pseudo-Goldstone boson as a dual photon. At the quantum phase transition, the model mimics some features of deconfined quantum criticality, but remains linearly confining. Deconfinement only sets in at high temperature.

Quantum link models (QLMs) are lattice gauge theories formulated in terms of discrete quantum degrees of freedom. $U(1)$ and $SU(2)$ QLMs were first constructed by Horn in 1981 [1], and further investigated in [2]. In [3] QLMs were introduced as an alternative non-perturbative regularization of Abelian and non-Abelian gauge theories, in which ordinary gauge fields emerge dynamically from the dimensional reduction of discrete quantum link variables. Dimensional reduction of discrete variables is a generic phenomenon in asymptotically free theories, which gives rise to the D-theory formulation of quantum field theory [4]. In the D-theory formulation of 4-d Quantum Chromodynamics (QCD), the confining gluon field emerges by dimensional reduction from a deconfined Coulomb phase of a $(4+1)$-d $SU(3)$ QLM [5]. Chiral quarks arise naturally as domain wall fermions located at the two 4-d sides of a $(4+1)$-d slab. The $(2+1)$-d $U(1)$ QLM has also been investigated in the context of quantum spin liquids [6]. With staggered background charges ± 1, it is equivalent to a quantum dimer model [7–9]. Furthermore, Kitaev's toric code [10] is a $\mathbb{Z}(2)$ QLM. In contrast to Wilson's lattice gauge theory [11], QLMs have a finite-dimensional Hilbert space per link, which makes them ideally suited for the construction of atomic quantum simulators for dynamical Abelian [12–16] and non-Abelian gauge theories [17–20]. A long-term goal of this research is to quantum simulate QCD in the D-theory formulation with ultracold matter, in order to address the real-time evolution of strongly interacting systems in nuclear and particle physics, as well as their dynamics at non-zero baryon density.

In this paper, we investigate the $(2+1)$-d $U(1)$ QLM, in order to demonstrate that, despite its structural simplicity, it displays highly non-trivial dynamics, and thus is ideally suited to demonstrate the power of gauge theory quantum simulators. We consider the model with a plaquette coupling J and a Rokhsar-Kivelson (RK) coupling λ. The phase diagram is sketched in Fig.1. At zero temperature, the model is confining for $\lambda < 1$. At finite temperature T, it has a deconfinement phase transition above which there is a massless mode transforming non-trivially under the $U(1)$ center symmetry. Due to the Mermin-Wagner theorem, this is not associated with spontaneous symmetry breaking. The deconfinement phase transition reaches zero temperature at the RK point, $\lambda = 1$. At λ_c there is a quantum phase transition which separates two phases with spontaneously broken translation symmetry [21]. The phase at $\lambda < \lambda_c$ has, in addition, a spontaneously broken charge conjugation symmetry. The two phases are similar to the columnar and plaquette ordered valence bond solid phases in a quantum dimer model [8], which may be separated by a first order phase transition [22] or by an intermediate phase [9].

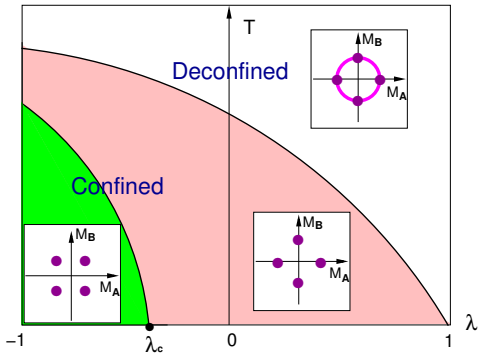

FIG. 1. [Color online] *Schematic sketch of the λ-T phase diagram. The insets indicate the location of the peaks in the probability distribution of the order parameter $p(M_A, M_B)$.*

As we will see, at λ_c a spontaneously broken approximate global $SO(2)$ symmetry emerges dynamically, giving rise to a light pseudo-Goldstone boson. The interface that separates the two broken phases on either side of the transition manifests itself as a string with fractional electric flux $\frac{1}{2}$. This raises the question whether the phase transition might be a deconfined quantum critical point in the sense of [23, 24], corresponding to a conformal field theory with an emergent massless photon and deconfined electric charges. Deconfined quantum criticality has first been investigated numerically in the J-Q quantum spin model [25–27], between an antiferromagnetic and a valence bond solid phase, and is still discussed controversially [28, 29]. It has also been studied in the J-Q [30]

and in the J_1-J_2 model [31–33] on the honeycomb lattice. At a deconfined quantum critical point, the instanton-like monopole events that cause permanent confinement in a $(2+1)$-d compact $U(1)$ gauge theory [34, 35] are eliminated, because a $\mathbb{Z}(4)$-invariant term that explicitly breaks the emergent $SO(2)$ symmetry of the effective action becomes irrelevant. We will see that this is not what happens in the $(2+1)$-d $U(1)$ QLM, where the $\mathbb{Z}(4)$-invariant term can be tuned to zero. Still, the emergent $SO(2)$ symmetry remains weakly explicitly broken by a "dangerously irrelevant" operator [36, 37]. This prevents the interpretation of the Goldstone boson as an emergent dual photon. It is more appropriate to think of it as an accidentally light Abelian "glueball". The dangerously irrelevant operator also contributes to the string tension and implies that the theory remains confining at the phase transition.

The Hamiltonian of the $(2+1)$-d $U(1)$ QLM is

$$H = -J \sum_{\square} \left[U_{\square} + U_{\square}^{\dagger} - \lambda (U_{\square} + U_{\square}^{\dagger})^2 \right]. \qquad (1)$$

Here $U_{\square} = U_{wx} U_{xy} U_{zy}^{\dagger} U_{wz}^{\dagger}$ is a plaquette operator formed by quantum links U_{xy} connecting nearest-neighbor sites x and y on a 2-d square lattice. A $U(1)$ quantum link $U_{xy} = S_{xy}^{+}$ is a raising operator of electric flux $E = S_{xy}^{3}$, constructed from a quantum spin $\vec{S}_{xy}$ associated with the link xy. In Wilson's lattice gauge theory, where the link variables are classical parallel transporters, $U_{xy} = \exp(i\varphi_{xy}) \in U(1)$, taking values in the gauge group, and $E_{xy} = -i\partial_{\varphi_{xy}}$, the single-link Hilbert space is infinite-dimensional. In the $U(1)$ QLM, on the other hand, it is just given by a finite-dimensional representation of the embedding algebra $SU(2)$. When one chooses spin $\frac{1}{2}$ on each link, the link Hilbert space is just 2-dimensional. The first term in the Hamiltonian flips a loop of electric flux, winding around an elementary plaquette, and annihilates non-flippable plaquette states, while the RK term, proportional to λ, counts flippable plaquettes. The Hamiltonian commutes with the generators, $G_x = \sum_i (E_{x,x+\hat{i}} - E_{x-\hat{i},x})$, of infinitesimal $U(1)$ gauge transformations. Here $\hat{i}$ is a unit-vector pointing in the i-direction. Physical states $|\Psi\rangle$ are gauge invariant, i.e. they obey the Gauss law $G_x|\Psi\rangle = 0$. Besides the gauge symmetry, the QLM also has several global symmetries, including lattice translation invariance and charge conjugation. Translation invariance characterizes each energy eigenstate by its lattice momentum $p = (p_1, p_2) \in]-\pi, \pi]^2$. Charge conjugation replaces U_{xy} by $U_{xy}^{\dagger}$ and E_{xy} by $-E_{xy}$, and characterizes each eigenstate by its charge conjugation parity $C = \pm$. Another important global symmetry is the center symmetry associated with "large" gauge transformations. The $U(1)$ QLM defined on a periodic volume has super-selection sectors characterized by wrapping electric fluxes that take values in $\mathbb{Z}/2$. On an $L_1 \times L_2$ lattice with periodic boundary conditions, the generators of the $U(1)$ center symmetry are $E_i = \frac{1}{L_i} \sum_x E_{x,x+\hat{i}}$. They commute with the Hamiltonian, but cannot be expressed through "small" periodic gauge transformations G_x.

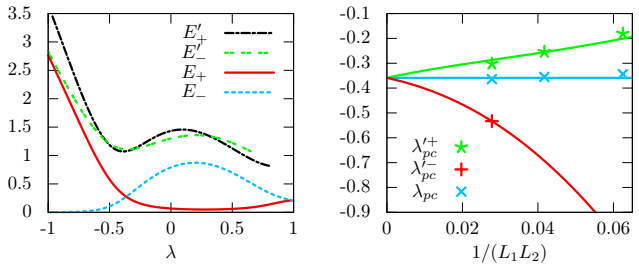

FIG. 2. [Color online] *a) Energy gaps of the lowest states on the* 6×6 *lattice as a function of* λ. *b) Global fit of* $L_1 L_2$*-dependence of* λ_{pc}, λ'^{+}_{pc}, *and* λ'^{-}_{pc}, *that yields* $\lambda_c = -0.359(5)$.

We have performed exact diagonalization studies of the $(2+1)$-d $U(1)$ QLM with $S = \frac{1}{2}$ on 4×4, 4×6, and 6×6 lattices. The energies of the lowest states are illustrated in Fig.2a. For $\lambda < 1$, the ground state has momentum $(0,0)$ and is even under charge conjugation (i.e. $C = +$). For $\lambda < \lambda_c$ the first excited state has quantum numbers $C = -$, $p = (\pi, \pi)$. Its energy gap to the ground state, $E_- \sim \exp(-\sigma_- L_1 L_2)$, decreases exponentially with the volume $L_1 L_2$, thus indicating the spontaneous breakdown of charge conjugation C and the translation T by one lattice spacing (in either direction). For $\lambda > \lambda_c$, another state $|C = +, p = (\pi, \pi)\rangle$ degenerates with the ground state, i.e. $E_+ \sim \exp(-\sigma_+ L_1 L_2)$, indicating that C is now restored, while T remains spontaneously broken. The crossing of the two excited energy levels, $E_-(\lambda_{pc}) = E_+(\lambda_{pc})$, defines a volume-dependent pseudo-critical coupling λ_{pc}. The next zero-momentum excited states, $|C = \pm, p = (0,0)\rangle$ with energies $E'_{\pm}$, cross twice near the critical point at two pseudo-critical couplings λ'^{+}_{pc} and λ'^{-}_{pc}, i.e. $E'_-(\lambda'^{\pm}_{pc}) = E'_+(\lambda'^{\pm}_{pc})$. As illustrated in Fig.2b, the couplings λ_{pc}, λ'^{+}_{pc}, and λ'^{-}_{pc} all approach $\lambda_c = -0.359(5)$ in the infinite volume limit.

The different symmetry breaking patterns are distinguished by two order parameters, M_A and M_B, associated with the even and odd dual sublattices A and B. A configuration of quantum height variables $h^A_{\widetilde{x}} = 0, 1$, $h^B_{\widetilde{x}} = \pm\frac{1}{2}$, located at the dual sites $\widetilde{x} = (x_1 + \frac{1}{2}, x_2 + \frac{1}{2})$, is associated with a flux configuration $E_{x,x+\hat{i}} = [h^X_{\widetilde{x}} - h^{X'}_{\widetilde{x}+\hat{i}-\hat{1}-\hat{2}}] \mathrm{mod} 2 = \pm\frac{1}{2}$, $X, X' \in \{A, B\}$. The two order parameters are given by $M_X = \sum_{\widetilde{x} \in X} s^X_{\widetilde{x}} h^X_{\widetilde{x}}$, where $s^A_{\widetilde{x}} = (-1)^{(\widetilde{x}_1 - \widetilde{x}_2)/2}$ and $s^B_{\widetilde{x}} = (-1)^{(\widetilde{x}_1 - \widetilde{x}_2 + 1)/2}$. Under C and T they transform as ${}^C M_A = M_A$, ${}^C M_B = -M_B$, ${}^T M_A = -M_B$, ${}^T M_B = M_A$. It should be pointed out that $\pm(M_A, M_B)$ represent the same physical configuration, because shifting the height variables to $h^X_{\widetilde{x}}(t)' = [h^X_{\widetilde{x}}(t) + 1] \mathrm{mod} 2$ leaves the electric flux configuration unchanged. We have performed quantum Monte Carlo sim-

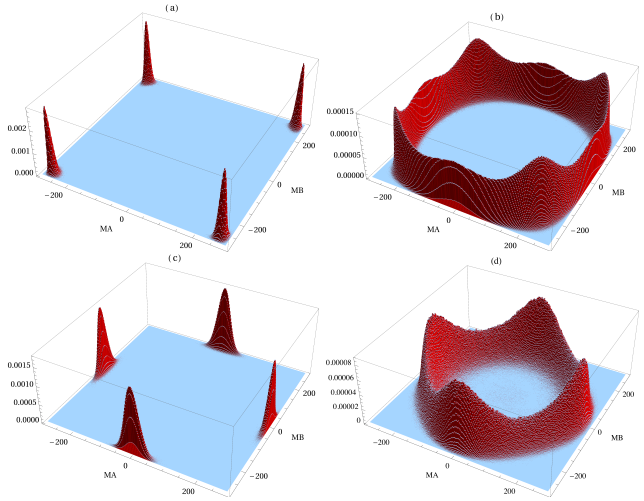

FIG. 3. [Color online] *Probability distribution* $p(M_A, M_B)$ *for* $\lambda = -1$, λ_c, *and 0 at* $T = 0$ *(a,b,c), and* $\lambda = 0$, $T > T_c$ *(d).*

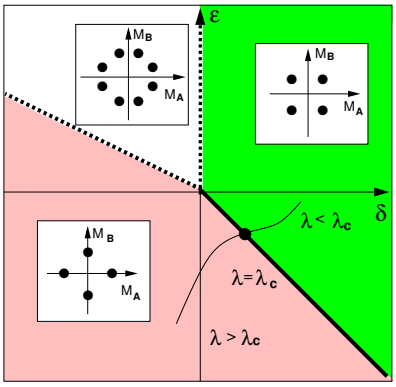

FIG. 4. [Color online] *Phase diagram as a function of* δ *and* ε. *The insets indicate the location of the peaks in the distribution* $p(M_A, M_B)$. *The fat and dashed lines are first and second order phase transitions, respectively. The curved line indicates a possible path taken in the QLM when varying* λ.

ulations with an efficient newly developed cluster algorithm, that will be described elsewhere. The algorithm has been used to determine the probability distribution $p(M_A, M_B)$ of the two order parameters M_A and M_B shown in Fig.3 at $\lambda = -1$, λ_c, and 0 for $L_1 = L_2 = 24a$, which reveals an emergent spontaneously broken $SO(2)$ symmetry at the quantum phase transition.

The low-energy effective theory describing the vicinity of the quantum phase transition is formulated in terms of a unit-vector field $\vec{e}(x) = (\cos\varphi(x), \sin\varphi(x))$ representing the direction of (M_A, M_B). Since (M_A, M_B) and $-(M_A, M_B)$ are indistinguishable, the effective theory is a $(2+1)$-d $\mathbb{R}P(1)$ model. Thus, only those states that are invariant against a sign-change of $\vec{e}(x)$ belong to the physical Hilbert space. Introducing $\partial_3 = \partial_{ct}$, the corresponding Euclidean effective action is

$$S[\varphi] = \int d^3x \frac{1}{c}\Big[\frac{\rho}{2}\partial_\mu\varphi\partial_\mu\varphi + \delta\cos^2(2\varphi) + \varepsilon\cos^4(2\varphi)\Big]. \quad (2)$$

Here ρ is the spin stiffness and c is the velocity of an emergent pseudo-Goldstone boson. $\delta + \varepsilon$ measures the deviation from the phase transition. The δ-term explicitly breaks the emergent $SO(2)$ symmetry to a $\mathbb{Z}(4)$ subgroup and gives rise to a small Goldstone boson mass $Mc = 2\sqrt{2|\delta|/\rho}$. Even when the relevant δ-term is tuned to zero, the dangerously irrelevant ε-term still explicitly breaks the $SO(2)$ symmetry. It is natural to define the dual field $F_{\mu\nu}(x) = \frac{1}{\pi}\varepsilon_{\mu\nu\rho}\partial_\rho\varphi(x)$. Since $\varphi(x)$ is well-defined only up to multiples of π, vortices and half-vortices in the order parameter field manifest themselves as charges. The electric charge contained in a spatial region Ω is given by twice the vortex number

$$Q_\Omega = \int_\Omega d^2x\ \partial_i F_{0i} = \frac{1}{\pi}\int_{\partial\Omega} d\sigma_i\ \varepsilon_{ij}\partial_j\varphi \in \frac{\mathbb{Z}}{2}. \quad (3)$$

Note that a charge 1 corresponds to a half-vortex, which is allowed because $\vec{e}(x)$ and $-\vec{e}(x)$ are physically equivalent. While the flux of $F_{\mu\nu}$ correctly represents the conserved charges of the $U(1)$ center symmetry, $F_{\mu\nu}$ should not be mistaken for a dual massless photon. This interpretation would require an exact $SO(2)$ symmetry, at least in the infrared. Due to the ε-term and other higher order symmetry breaking terms, this would require a large amount of fine-tuning.

By applying the Ginsburg-Landau-Wilson paradigm to the δ- and ε-terms, in mean field theory one obtains the phase diagram of Fig.4. The two phases realized in the QLM both have four peaks in the order parameter distribution $p(M_A, M_B)$, and are separated by a weak first order phase transition. In addition, there is an intermediate phase with eight peaks (whose analog may be realized in the quantum dimer model [9]), separated from the other phases by second order phase transitions [36]. If one would fine-tune to these transitions, the Goldstone boson would become exactly massless. Even then it could not be interpreted as a dual photon, because the $SO(2)$ symmetry would still remain explicitly broken.

The effective theory predicts a finite-volume rotor spectrum ($E_m = m^2c^2/(2\rho L_1 L_2)$ when $\delta = \varepsilon = 0$) with $m = 0, \pm2, \pm4, \ldots$ States with odd values of m are excluded because they are not invariant against a sign-change of $\vec{e}(x)$. The quantum numbers of the states with $m = 0, \pm2, \pm4$ correspond to $C = +, p = (0,0)$, $C = \pm, p = (\pi,\pi)$, $C = \pm, p = (0,0)$, respectively. The effective theory is in quantitative agreement with the exact diagonalization study (cf. Fig.2b). A global fit of the energy spectrum yields $\lambda_c = -0.359(5)$, $\rho = 0.45(3)J$, $c = 1.5(1)Ja$, $\delta_c = -\varepsilon_c = 0.01(1)J/a^2$. A more precise determination of the low-energy constants and of λ_c, based on high accuracy Monte Carlo simulations using the cluster algorithm, will be presented elsewhere.

Away from the critical point, the δ-term gives rise to two distinct coexisting phases that are related by C and T

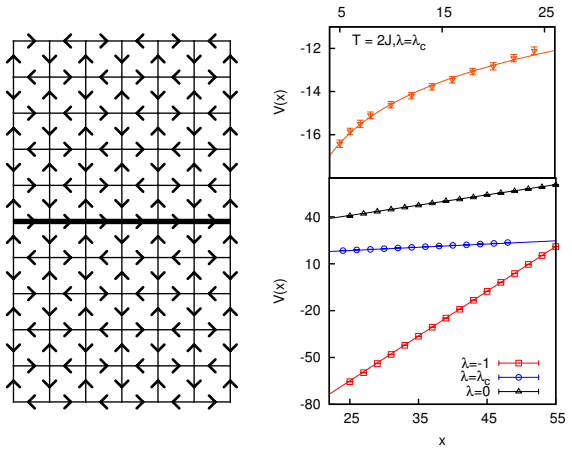

FIG. 5. [Color online] *a) Interface at $\lambda \to -\infty$. The fat line is a flux $\frac{1}{2}$ string. b) Potential between two static charges ± 2 separated by the distance (x, x) along a lattice diagonal, for $\lambda = -1, \lambda_c$, and 0, at $T = 0$, and at $\lambda = \lambda_c$ for $T = 2J$.*

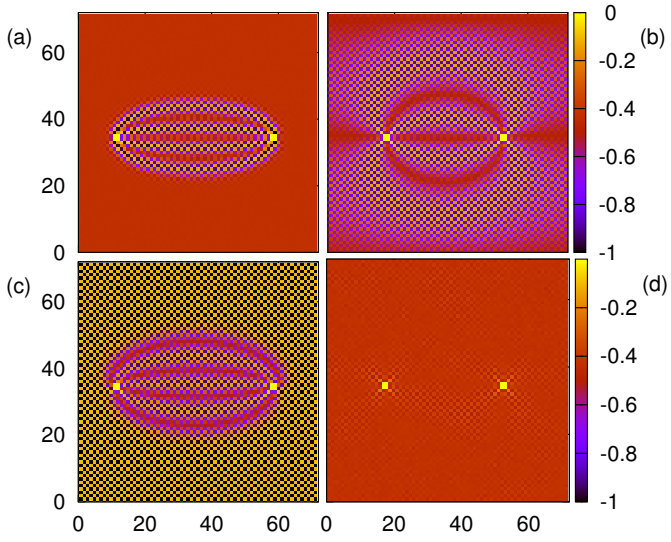

FIG. 6. [Color online] *Energy density $-J\langle U_\Box + U_\Box^\dagger\rangle$ in the presence of two charges ± 2 for $\lambda = -1$ (a), $\lambda = \lambda_c$ (b), and $\lambda = 0$ (c) at $T = 0$, as well as for $\lambda = 0$ at $T > T_c$ (d).*

for $\lambda < \lambda_c$, and by T for $\lambda > \lambda_c$. As illustrated schematically in Fig.5a for $\lambda \to -\infty$, the interface that separates the two phases represents a string of electric flux $\frac{1}{2}$. Its interface tension, $\sigma_{1/2} = \sqrt{2|\delta|\rho}$ (for $\varepsilon = 0$), which plays the role of a string tension, would vanish at the phase transition if there was no ε-term. While the ε-term would simply be irrelevant at a critical point, here it is dangerously irrelevant. Taking it into account, the string tension never vanishes, and is always of order $\sqrt{\rho\varepsilon}$. Indeed, the potential (shifted by a constant) between two static charges ± 2, illustrated in Fig.5b, shows linear confinement at large distances, even at the phase transition, albeit with a small string tension $\sigma_2 = 0.201(2)J/a$ (compared to $\sigma_2 = 1.97(1)J/a$ at $\lambda = -1$). This shows explicitly that the phase transition is not a deconfined quantum critical point. The energy density $-J\langle U_\Box + U_\Box^\dagger\rangle$ in the presence of two charges ± 2 is illustrated in Fig.6a-d. The flux string connecting the charges separates into four strands of flux $\frac{1}{2}$ that repel each other. In accordance with the effective theory, the interior of the strands consists of the phase that is stable on the other side of the transition. Near λ_c the flux string undergoes topology change by wrapping one strand over the periodic boundary and materializing an additional strand at the edge of the system, whose interior then expands to become the new bulk phase (cf. Fig. 6b). Viewed as interfaces separating bulk phases, the strands display the universal phenomenon of complete wetting.

Finally, we have studied the system at finite temperature. The electric flux susceptibility, $\langle E_i^2\rangle$ is non-zero at $T > T_c$, indicating a massless mode that transforms non-trivially under the $U(1)$ center symmetry, giving rise to a logarithmic charge-anti-charge potential (c.f. Fig.5b). Hence, the "deconfined" phase no longer has linear, but still has logarithmic confinement. As illustrated in Fig.6d, the flux then spreads out and no longer forms a string. Interestingly, the shift symmetry T remains spontaneously broken at high temperature (c.f. Fig.3d). Actually, in the deconfined phase yet another $SO(2)$ symmetry emerges, which originates from the Gauss law.

In conclusion, we have observed an emergent $SO(2)$ symmetry with an associated pseudo-Goldstone boson in the (2+1)-d $U(1)$ QLM. Interfaces separating phases with spontaneously broken C or T symmetry manifest themselves as strings carrying fractional electric flux $\frac{1}{2}$. Although the model displays certain features of deconfined quantum critical points, a dangerously irrelevant operator leads to small explicit $SO(2)$ breaking. This prevents the interpretation of the emergent Goldstone boson as a massless photon, and implies a non-zero string tension also at the phase transition. It remains to be seen whether phenomena, similar to the ones observed in the QLM, may masquerade as deconfined quantum criticality in other models as well. Once the $(2+1)$-d $U(1)$ QLM is realized in ultracold matter experiments, its rich dynamics will become accessible to quantum simulation.

We dedicate this work to the memory of Bernard B. Beard. He is deeply missed, not only as a collaborator, who would have elegantly performed all simulations in this paper in continuous time [38]. We like to thank W. Bietenholz, M. Dalmonte, C. P. Hofmann, E. Katz, A. Läuchli, M. Lüscher, F. Niedermayer, G. Palma, E. Rico, A. Sen, and P. Zoller for illuminating discussions. UJW acknowledges B. B. Beard, R. Brower, S. Chandrasekharan, V. Chudnovsky, U. Gerber, M. Pepe, and A. Tsapalis for their collaboration on previous attempts to simulate quantum links. This research has been supported by the Schweizerischer Nationalfonds.

[1] D. Horn, Phys. Lett. 100B (1981) 149.
[2] P. Orland, D. Rohrlich, Nucl. Phys. B338 (1990) 647.
[3] S. Chandrasekharan, U.-J. Wiese, Nucl. Phys. B492 (1997) 455.
[4] R. Brower, S. Chandrasekharan, S. Riederer, U.-J. Wiese, Nucl. Phys. B693 (2004) 149.
[5] R. Brower, S. Chandrasekharan, U.-J. Wiese, Phys. Rev. D60 (1999) 094502.
[6] M. Hermele, M. P. A. Fisher, L. Balents, Phys. Rev. B69 (2004) 064404.
[7] D. S. Rokhsar and S. A. Kivelson, Phys. Rev. Lett. 61 (1988) 2376.
[8] R. Moessner, S. L. Sondhi, E. Fradkin, Phys. Rev. B65 (2002) 024504.
[9] A. Ralko, D. Poilblanc, R. Moessner, Phys. Rev. Lett. 100 (2008) 037201.
[10] A. Kitaev, Ann. Phys. 321 (2006) 2.
[11] K. Wilson, Phys. Rev. D10 (1974) 2445.
[12] H. P. Büchler, M. Hermele, S. D. Huber, M. P. A. Fisher, P. Zoller, Phys. Rev. Lett. 95 (2005) 040402.
[13] E. Zohar, J. Cirac, B. Reznik, Phys. Rev. Lett. 109 (2012) 125302.
[14] D. Banerjee, M. Dalmonte, M. Müller, E. Rico, P. Stebler, U.-J. Wiese, P. Zoller, Phys. Rev. Lett. 109 (2012) 175302.
[15] L. Tagliacozzo, A. Celi, A. Zamora, M. Lewenstein, Ann. Phys. 330 (2013) 160.
[16] E. Zohar, J. Cirac, B. Reznik, Phys. Rev. Lett. 110 (2013) 055302.
[17] D. Banerjee, M. Bögli, M. Dalmonte, E. Rico, P. Stebler, U.-J. Wiese, P. Zoller, Phys. Rev. Lett. 110 (2013) 125303.
[18] E. Zohar, J. Cirac, B. Reznik, Phys. Rev. Lett. 110 (2013) 125304.
[19] L. Tagliacozzo, A. Celi, P. Orland, M. Lewenstein, arXiv:1211.2704.
[20] E. Zohar, J. Cirac, B. Reznik, arXiv:1303.5040.
[21] N. Shannon, G. Misguich, K. Penc, Phys. Rev. B69 (2004) 220403.
[22] A. Vishwanath, L. Balents, T. Senthil, Phys. Rev. B69 (2004) 224416.
[23] T. Sentil, A. Vishwanath, L. Balents, S. Sachdev, M. P. A. Fisher, Science 303 (2004) 1490.
[24] T. Sentil, L. Balents, S. Sachdev, A. Vishwanath, M. P. A. Fisher, Phys. Rev. B70 (2004) 144407.
[25] A. W. Sandvik, Phys. Rev. Lett. 98 (2007) 227202.
[26] R. G. Melko, R. K. Kaul, Phys. Rev. Lett. 100 (2008) 017203.
[27] F.-J. Jiang, M. Nyfeler, S. Chandrasekharan, U.-J. Wiese, J. Stat. Mech. (2008) P02009.
[28] K. Chen, Y. Huang, Y. Deng, A. B. Kuklov, N. V. Prokof'ev, B. V. Svistunov, arXiv:1301.3136.
[29] Y. Tang, A. W. Sandvik, arXiv:1301.3207.
[30] K. Damle, F. Alet, S. Pujari, arXiv:1302.1408.
[31] A. F. Albuquerque, D. Schwandt, B. Hetenyi, S. Capponi, M. Mambrini, A. M. Läuchli, Phys. Rev. B84 (2011) 024406.
[32] Z. Zhu, D. A. Huse, S. R. White, arXiv:1212.6322.
[33] R. Ganesh, J. van den Brink, S. Nishimoto, arXiv:1301.0853.
[34] A. M. Polyakov, Phys. Lett. B59 (1975) 82; Nucl. Phys. B120 (1977) 429.
[35] M. Göpfert, G. Mack, Commun. Math. Phys. 82 (1982) 545.
[36] A. D. Bruce, A. Aharony, Phys. Rev. B11 (1975) 478.
[37] D. J. Amit, L. Peliti, Ann. Phys. 140 (1982) 207.
[38] B. B. Beard, U.-J. Wiese, Phys. Rev. Lett. 77 (1996) 5130.